Plankton and Particle Size and Packaging: From Determining Optical Properties to Driving the Biological Pump

L. Stemmann[1] and E. Boss[2]

[1]Université Pierre et Marie Curie (UPMC), Paris 06, UMR 7093, Observatoire Océanographique (LOV), F-06234 Villefranche/Mer, France; email: stemmann@obs-vlfr.fr

[2]School of Marine Sciences, University of Maine, Orono, Maine 04469-5706

Annu. Rev. Mar. Sci. 2012. 4:263–90

First published online as a Review in Advance on October 13, 2011

The *Annual Review of Marine Science* is online at marine.annualreviews.org

This article's doi: 10.1146/annurev-marine-120710-100853

1941-1405/12/0115-0263$20.00

Keywords

marine particles, biological pumps, size distribution

Abstract

Understanding pelagic ecology and quantifying energy fluxes through the trophic web and from the surface to the deep ocean requires the ability to detect and identify all organisms and particles in situ and in a synoptic manner. An idealized sensor should observe both the very small living or dead particles such as picoplankton and detritus, respectively, and the large particles such as aggregates and meso- to macroplankton. Such an instrument would reveal an astonishing amount and diversity of living and nonliving particles present in a parcel of water. Unfortunately such sensors do not exist. However, complex interactions constrain the space, temporal, and size distributions of these objects in such ways that general rules can be inferred from the measurement of their optical properties. Recent technological developments allow for the in situ measurement of the optical properties and size distributions of particles and plankton in a way such that synoptic surveys are possible. This review deals with particle and plankton size distributions (PSDs) as well as how particles' geometry and nature affect their optical properties. Finally, we propose the integration of the PSD into size-structured mathematical models of biogeochemical fluxes.

INTRODUCTION

A central goal of biological oceanography during the past two decades has been to understand the factors that control the fate of particulate organic matter produced in the ocean mainly to quantify the vertical flux of carbon to the deep sea. In the open ocean, the first building blocks of organic particles can be produced through different pathways among which primary production is the most important. Thereafter, zooplankton of increasing size consume these particles and produce other particles, leading to the production of larger detritus as waste products of the pelagic ecosystem functioning (fecal pellets, molts, dead bodies) (Alldredge & Silver 1988, Sheldon et al. 1972). A second pathway consists of the direct physical coagulation of phytoplankton cells and other particles into larger aggregates (Jackson 1990, McCave 1984). Transparent exopolymer particles are major agents in the aggregation of particles binding the different constituents into marine snow particles (Alldredge et al. 1993). Opposed to the aggregation processes, other processes such as bacterial solubilization and zooplankton activities or physical fragmentation tend to reduce particle size. Therefore, observed particle size distributions generally reflect the net result of aggregation and disaggregation processes.

Dominant processes that affect particle concentrations include production, coagulation, consumption/solubilization, and settling. Size is an important particle property affecting all these processes. Particle diameter can be a determinant of multiple physical properties such as settling speed or flux (Alldredge & Gotschalk 1988), coagulation rate (Jackson 1990, McCave 1984), biological properties such as the rate of colonization and use by microbes and zooplankton (Kiørboe 2000; Kiørboe et al. 2002, 2004), and biogeochemical activity such as aggregate remineralization by bacterial activity or zooplankton consumption (Kiørboe & Thygesen 2001, Ploug & Grossart 2000, Ploug et al. 2008a). In addition, many ecological traits (including population abundance; growth rate and productivity; as well as trophic, competitive, and facilitative relationships between species) as well as metabolic processes are correlated with body size (Brown et al. 2004; Gillooly 2000; Gillooly et al. 2001, 2002). Furthermore, because most marine organisms are highly opportunistic feeders and because prey size is limited by the allometric diameter of a predator's mouth, predator-prey relationships can be, in many marine systems, determined by size (Hansen et al. 1997, Jennings & Warr 2003). In addition, a predator's ability to visually detect prey is dependent on the available light (Aksnes et al. 2004, Sornes et al. 2008), which in turn is primarily dependent on light absorption by particles. Hence, because the size of organisms or particles captures so many aspects of ecosystem functioning, it can be used to synthesize a suite of covarying traits into a single dimension (Woodward et al. 2005).

Ocean carbon sources and sinks are controlled by both physical and biological processes that act at various temporal and spatial scales. Based on global biogeochemical modeling and on the use of paleoproxies from sedimentary archives, the surface production and downward settling of biogenic particulate matter from the euphotic zones of the ocean to the deep sea and ultimately to the sediment—a process termed the biological carbon pump (Volk & Hoffert 1985)—contribute significantly to climate variability (Sarmiento & Le Quere 1996). However, the uncertainties in our understanding of the biological pump's functioning in today's oceans remain important. Recent reviews about the export of biogenic particles to the deep ocean showed that there is no consensus regarding the mechanisms controlling its spatial and temporal variability (Boyd & Trull 2007). Observing particle and plankton size distributions (PSDs) in a synoptic manner could help to better understand the processes contributing to the biological pump. Novel sensors have provided in situ information that was not available beforehand to understand and quantify the functioning of the biological pump (Finlay et al. 2007; Gallienne & Robins 1998; Gallienne et al. 2001; Gorsky et al. 1992b; Herman et al. 2004;

Huntley et al. 1995; Stemmann et al. 2002, 2008b). Great improvement in our knowledge of pelagic ecosystems is, therefore, expected in the next decade because these instruments are miniaturized and could eventually be used on autonomous platforms (Johnson et al. 2009), increasing significantly the temporal and spatial coverage of such measurements.

The scope of this review is to provide insights into the impact of particle size on the light field in the sea and the dynamics of particles and plankton as revealed by the measurement of their size. This review deals with particle and plankton size distributions, the impact of particles' packaging and composition on their optical properties, new or recent in situ instruments, and the need for global observation of PSD. Finally, we propose the integration of PSD into mathematical models of biogeochemical fluxes.

CONCEPTUAL MODELS FOR PARTICLE AND ZOOPLANKTON SIZE DISTRIBUTION

From the sensor's perspective, any detected object is a particle, living or not. Living particles can be heterotrophic bacteria, phytoplanktonic, protozoa, and larger zooplanktonic organisms. For clarity, throughout this review, the term PSD is used for nonliving and living particles unless otherwise specified; particle is used to indicate phytoplankton cells as well as individual nonliving particles and aggregates, excluding metazoan organisms. A convenient way to analyze the size properties of plankton and particles is to first sort them according to their size and then compute a size-distribution histogram. Size can be expressed in terms of many descriptors such as length, volume, mass, carbon content, etc. This section presents the conceptual and mathematical frameworks used to calculate the size spectra of zooplankton and particles, following numerous other works (Gaedke 1992, Huntley et al. 1995, Jackson et al. 1997, Jennings et al. 2007, Martin et al. 2006, McCave 1984, Milligan 1996, Sprules & Munawar 1986, Vidondo et al. 1997, Zhou & Huntley 1997). In the discussion below, the term size usually refers to diameter (d) as determined from images, and in most cases, this diameter is measured as the equivalent spherical diameter (ESD, the diameter of a sphere of equivalent volume).

Conceptual Model for Particle Size Distribution

Particles range from individual cells through chains to assemblages of highly degraded detritus forming aggregates; they can be formed directly by biological processes such as cell division and fecal pellet production or indirectly by coagulation of particles due to differential settling and turbulence. Marine aggregates are a key factor in the ocean's carbon cycle at different scales. At the macroscale, marine aggregates are an important means of transferring carbon downward to depth by way of sinking (as they sink faster than their component particles). At the microscale, they provide dissolved and particulate food to micro- and macro-organisms living in the aphotic layer of the ocean (Alldredge 2000, Lampitt 1992, Lampitt et al. 1993). Aggregates are an especially important nutritional source for benthic communities, which are the ultimate recipients of the flux (Smith et al. 2009).

Particles found in oceanic ecosystems range in diameter from 1 nm (almost-dissolved colloids) to a few millimeters (diatom chains) or centimeters (cyanobacterial filaments). Three size classes of organic aggregates have often been distinguished in the past: macroscopic aggregates ($d > 500$ μm) (typically, marine snow), microscopic aggregates ($1 < d < 500$ μm) (also known as microaggregates), and submicron particles ($d < 1$ μm) (Simon et al. 2002). Their sizes can depend on the trophic state of the planktonic system, on the season, and on the geographic region. Their composition is very complex and can vary from being individual algal cells to being

composed of multiple particles (such as zooplankton feces or molts or mineral material) embedded in a mucilaginous matrix (Alldredge & Gotschalk 1988). The large size range covered by these organic aggregates implies that many complex physical, chemical, biological, and specific microbial processes are involved in their formation and decomposition (Alldredge & Silver 1988). Most aggregates are fragile, making obtaining their size measurement difficult because either handling or the flow associated with instruments disrupts their structure (Gardner et al. 2003). Hence, the best instruments for measuring their size are those that make measurements in situ in undisturbed water.

PSD is usually estimated by counting the number of particles within a given particle length range and dividing that number by the length range and by the volume of water sampled. Because size can be measured with optical techniques, many marine particle studies measure particle distribution as a function of length such as, for example, the ESD based on optical cross-section or electrical resistivity (Jackson et al. 1995, Stemmann et al. 2008a). However, for aggregates, this relationship is not simple because of their inherent heterogeneity. First, aggregates have a significant water fraction, which increases with their size, and second, many aggregates are formed from different components, each with a different density. The measures of particle size depend on the measurement techniques, which measure different physical properties, making size comparisons very difficult. Accurate and homogeneous particle size measurements are nevertheless required to use PSDs as ecological indicators. Therefore, careful experiments and mathematical frameworks must be developed. For example, a Coulter counter measures the change in electrical resistance when a particle passes through an orifice. The resistance is approximately proportional to the solid particle volume (the conserved volume) and excludes any water between the solid parts of an aggregate. The diameter of a sphere with such a conserved volume is the conserved diameter, d_c. The diameter of the overall object including any contained water is the fractal diameter, d_f (which is called the apparent diameter). The two values are related using fractal scaling (Jackson 1990). For a solid object, the two diameters are the same. If the particle is porous, as in a marine aggregate, they can be very different. Knowledge of this property is of the utmost importance to convert the size into volume and mass (Jackson et al. 1997, Stemmann et al. 2008a) and to predict settling rates. If the aggregates are opaque, some of their optical properties (e.g., near-forward angular scattering) are similar to those of dense particles and, hence, can be inverted to obtain the size of the aggregates (e.g., with Sequoia Scientific's LISST). By contrast, other optical properties, such as the beam attenuation, are well correlated with dry mass in coastal or estuarine systems (Boss et al. 2009b; see also recent review in Hill et al. 2011). Hence, the ratio of beam attenuation to volume can be used to obtain a bulk packaging parameter, as has been demonstrated recently in controlled laboratory aggregation experiments and manipulation experiments of particles in coastal waters (Slade et al. 2011). Comparing PSDs from different instruments and across different types of marine systems is still in its infancy (e.g., Mikkelsen et al. 2006), and more experimental studies are needed.

Conceptual Model for Zooplankton Size Distribution

As for particles, there are many ways to characterize zooplankton size. Typically, zooplankton have been divided into size groups that are operationally determined on the basis of the mesh size of a net: Microzooplankton ($20 < \text{size} < 200$ μm) includes protozoa, larvae, and juveniles of metazoa; mesozooplankton ($200 < \text{size} < 2{,}000$ μm) is mostly metazoa with the dominant group of copepods; and macrozooplankton (size $> 2{,}000$ μm) is constituted mainly of metazoa with the dominant group of decapods and jelly plankton (tunicates, cnidarians). Most previous work using automated counting systems has used a single descriptor of size, such as the diameter, because

the shapes were not well resolved with these systems. However, most of these organisms are not spherical and have very diverse morphologies, making it meaningless to calculate length based on a single common measurement. Assuming a spherical shape tends to overestimate size because the ratio of volume to projected cross-sectional area is greater for spheres than for other shapes (Beaulieu et al. 1999, Sprules et al. 1998). By chance for the scientist, the most numerically abundant metazoan organisms in the plankton are copepods, an organism that may be represented using a spheroid (Herman 1992). To calculate the biovolume of a spheroid from a recorded shadow area, it is necessary to know the ratio of its major and minor axes and its orientation relative to the beam.

A few imaging systems now provide reliable in situ estimates of the length (often called major) and width (often called minor). In the case of zooplankton, the most commonly used framework in analyzing zooplankton size distribution has been called the normalized biomass spectrum, which is the total biomass in a size interval normalized by the width of the size interval and the sampled volume (Platt & Denman 1978). As for the particle abundance spectrum, the biomass spectrum is well defined for a given size-structured plankton community and independent of the subjective-sorting size intervals. Significant efforts have been made to interpret the meaning of biomass spectrum slopes in terms of growth, mortality, respiration, and survival by both empirical and theoretical relationships (Platt & Denman 1978, Zhou 2006, Zhou & Huntley 1997).

Common Mathematical Model for Living and Dead Particles

Dealing with millions of size spectra requires using simple mathematical description as a start. The differential particle or plankton size distribution (n, particle number cm^{-3} cm^{-1}), also called the particle size spectrum (Burd & Jackson 2009), is a useful description of the relationship between a given organism or particle abundance and size. This relationship is generally approximated by a two-parameter power-law function:

$$n = bd^{-k}, \tag{1}$$

where b is a constant, k the slope (in log-log form), and d the particle or organism diameter. The differential particle abundance, $n = \mathrm{d}N/\mathrm{d}d$, can be calculated from $\mathrm{d}N$, the total number of objects per unit volume in a diameter range between d and $d + \mathrm{d}d$, where $\mathrm{d}d$ is a small diameter increment.

The exponent (k) is also defined as the slope of the spectrum when Equation 1 is log transformed. This slope is commonly used as a descriptor of the shape of the aggregate size distribution (Brun-Cottan 1971, McCave 1983, McCave 1984, Sheldon et al. 1972, Stemmann et al. 2000, Stemmann et al. 2002). The information of this simple metric can be biased when the log-transformed spectrum is not linear. The importance of large aggregates in some systems can be missed if only the slope of a defined spectrum is used (e.g., Jackson et al. 1995).

Figure 1 presents the PSD ($3 < d < 100$ μm) estimated using the HIAC/Royco particle counter (Pacific Scientific Instruments) after collection of large particles (60 μm $< d <$ 1 cm) measured in situ by the Underwater Vision Profiler (UVP) (Picheral et al. 2010) and of zooplankton collected by a WP2 net [Working Party net with a mesh size of 200 μm (Harris et al. 2000)] in the upper 200 m of the water column during the BIOSOPE cruise across the south tropical Pacific (Stemmann et al. 2008a). The HIAC/Royco and UVP count have been integrated in the same layer. To assess the contribution of living particles to the total PSD, zooplankton size distributions were calculated on images obtained from the ZooScan imaging system (Gorsky et al. 2010). Zooplankton organisms were separated from all particles collected in the net using automatic pattern recognition followed by validation as described in Gorsky et al. (2010). The number distributions follow roughly the same linear decrease on a log-log plot and with a slope close to −4. Despite the relatively simple nature of the PSD and the fitting with a slope, the volume distribution is more variable with

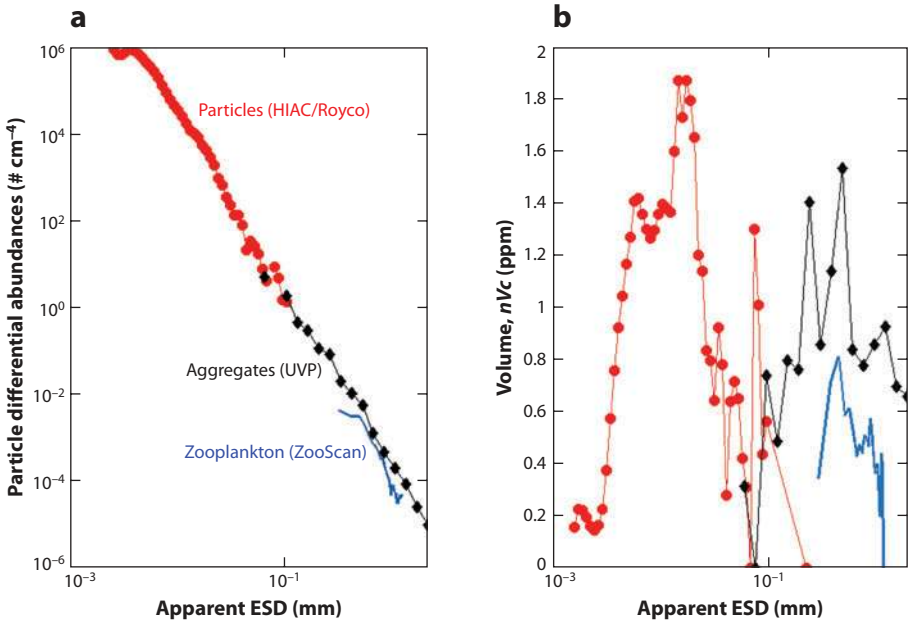

Figure 1

(*a*) Average particle and zooplankton differential abundance and (*b*) differential volume distributions in the upper 200-m depth from the HIAC/Royco particle counter, the Underwater Vision Profiler (UVP), and the ZooScan system in the oligotrophic central South Pacific Gyre (GYR site). The volume distributions have been calculated as in Stemmann et al. (2008a). These distributions were calculated using the apparent particle diameters reported by the instruments and the converted apparent diameter from the conserved diameter given by the HIAC/Royco counter. The slope of the number distribution is approximately −4. Abbreviation: ESD, equivalent spherical diameter.

two peaks because what are small deviations from the straight line in a log-log plot become large variations in the volume estimates. In addition, the volume estimates are very sensitive to crucial parameters such as the fractal dimension and the particular organic carbon (POC)/dry weight ratio (Stemmann et al. 2008a). Aggregates are several times more abundant than zooplankton and show more volume. The volume distribution shows a larger volume fraction of aggregates >1 mm. These aggregates could be observed on the video image and were probably living organisms (Stemmann et al. 2008a). They were not observed in the net, showing how variable the plankton census is when using different instruments. It is most probable that large differences in abundance between detritus and living organisms are common in the seas (see Differentiating Between Dead and Living Particles, below).

Because trophic currency is mass (e.g., carbon or nitrogen) rather than number, the size distribution expressed in terms of length can be converted to biomass based on the mass-length relationship. For particles, the conserved volume (V) is often calculated from d_c (conserved diameter, see above), assuming a sphere:

$$V = 4/3\pi(d_c/2)^3. \quad (2)$$

For zooplankton and, specifically, copepods, the ellipsoid volume is often estimated using the following equation:

$$V = 4/3\pi b^2 a, \quad (3)$$

where b is the minor and a is the major axis. The total mass M or dry weight can also be calculated knowing the density (ρ) of the matter in the volume:

$$M = \int_0^\infty n_c \rho V dv. \quad (4)$$

The values of particle dry weight can be converted to POC assuming POC = 20% to 50% dry weight (Alldredge 1998) and compared with independent POC measurements. For zooplankton, numerous other algorithms exist (Harris et al. 2000).

MEASURING PARTICLE AND PLANKTON SIZE USING OPTICAL TECHNOLOGIES

Effects of Particle Size on Their Measured Optical Properties

Optical methods are currently the only in situ methods to measure the size of micron-sized particles. Light absorption depends on the properties of the particles (e.g., size, shape, pigment concentration) as well as the nature and quantity of the available subsurface light. Underwater visibility depends on the underwater light distribution, which is determined by the underwater optical properties (absorption, polarized scattering, and fluorescence), which are themselves determined by the concentration, size, shape, packaging, and composition of particulate and dissolved materials in the water. In addition, the "quality" of the light—e.g., its polarization properties—has been found to be important to many visual marine species, who are sensitive to polarization (Cronin et al. 2003).

To first order, optical properties respond to particle concentration. For example, POC concentrations vary by approximately 3 orders of magnitude in the surface ocean [from 15 mg to 2,000 mg m^{-3} (D. Stramski, personal communication)]; hence, optical properties span a similar range of magnitudes. Beyond concentration, the next most important determinants of optical properties are size and packaging (degree of aggregation, fluid fraction) and composition (index of refraction), though the latter is less important for particles significantly larger than the wavelength (see below). Shape also modulates optical properties, but within a range that is usually significantly smaller than the above properties, except perhaps for the backscattering coefficient (Clavano et al. 2007).

The size of matter that significantly affects optical properties varies by 12 orders of magnitude, from water molecules and dissolved salts to large aggregates (**Figure 2**). Size boundaries for optical regions are defined on the basis of theoretical consideration of light interactions with particles given the physical properties of the particle, the medium in which it is immersed, and the wavelength of light.

The interaction of light with particles is particularly sensitive to the ratio of size to wavelength, $x \equiv \pi d/\lambda$, where λ is the wavelength of the light in the medium in which the particle is immersed, e.g., water; x, termed the size parameter, is used to define different regions where the interaction of light with matter has particular and predictable characteristics (van de Hulst 1981). The two simplest regions are that of Rayleigh ($x \ll 1$), where the angular scattering is symmetric about 90°, scattering is strongly dependent on wavelength (proportional to λ^{-4}), and shape does not matter, and that of geometric optics ($x \gg 1$), where most of the light is scattered very close to near forward, attenuation does not depend on wavelength, and shape (particularly the average-cross-sectional area to volume ratio) matters. In between these two regimes, there is a transition zone where some analytical solutions exist (e.g., the anomalous diffraction approximation; van de Hulst 1981). Attenuation per mass in that region has a maxima for particle with a phase-shift parameter,

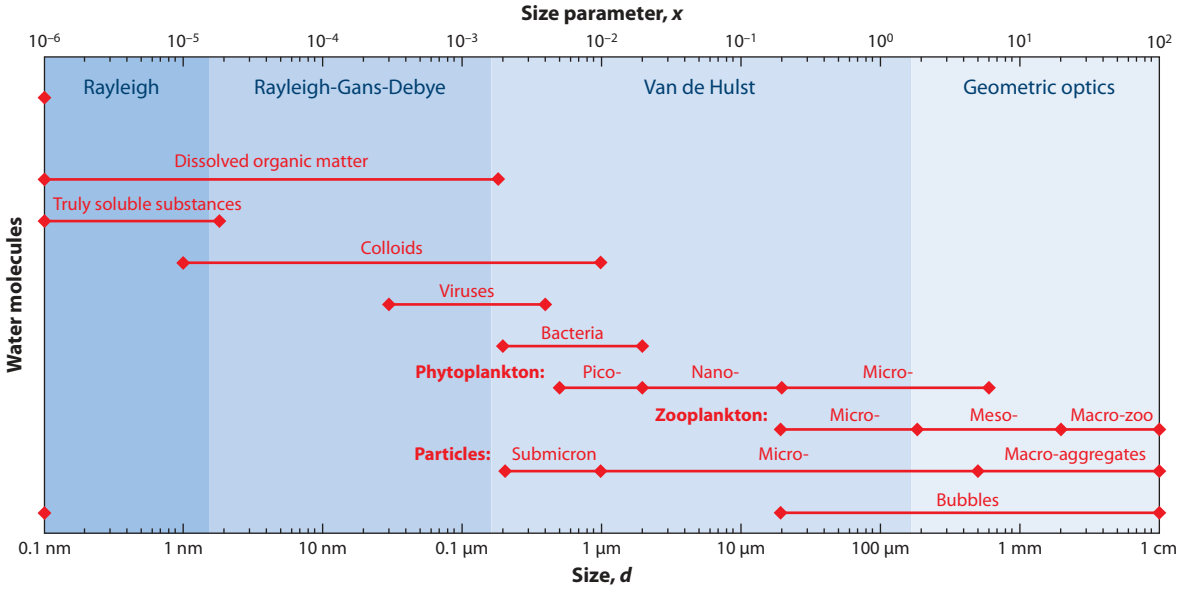

Figure 2

Representative sizes of different constituents in seawater (based on Clavano et al. 2007, Stramski et al. 2004). Different optical regions are denoted by different shading, as a function of size (lower x axis) and size parameter (x, upper x axis, assumes $\lambda = 400$ nm). The boundaries between the regions are not exact and vary with the complex index of refraction for a given particle size.

ρ, defined as $\rho \equiv 2x(n-1) \sim 3$ (analytical result based on the anomalous diffraction approximation; van de Hulst 1981), with the major contribution to attenuation coming from $5.5 > \rho > 1$ (**Figure 3**), where n is the real part of the index of refraction relative to the medium (oceanic particles have $1.2 > n > 1.02$, with water content playing an important role; Aas 1996). In terms of diameter, the half-max width from which the majority of contribution comes is $5.5\lambda/[2\pi(n-1)] > d > \lambda/[2\pi(n-1)]$ [hence, for sediments ($n \sim 1.17$) at $\lambda_{air} = 650$ nm, that is, 2.5 µm > d > 0.46 µm, whereas for phytoplankton-like particles at the same wavelength ($n \sim 1.05$) 8.5 µm > d > 1.5 µm].

Absorption per mass decreases with size as a result of the reduction in the interaction of light with absorbing matter within the particle compared with the interaction with absorbing material near the particle's surface (referred to as the package effect) (Duysens 1956, Morel & Bricaud 1981). Note that in this review we use packaging as a descriptor of aggregation state (**Figure 4**). Rather than ρ, the parameter that dominates absorption is the product $x \cdot n'$, where n' is the imaginary part of the index of refraction. For dissolved material ($d \ll \lambda$), absorption is given by $a = 4\pi n'/\lambda$. Variation in the index of the real part of the index of refraction changes absorption by only ±15%, and the package effect becomes important (reduction of 50% in absorption) at $x \cdot n' \sim 0.8$, that is, for $d \sim 0.25\lambda/n'$ (**Figure 3**).

Aggregate Particle Optics: Effects of Size and Packaging

The simplest analytical result for light interaction with a particle in the intermediate range where scattering per mass is maximal is that of the anomalous diffraction approximation (van de Hulst 1981), which provides a good prediction for soft particles (where $n \sim 1$, as for most aquatic particles). Because during aggregation the bulk index of refraction of aggregates decreases as their

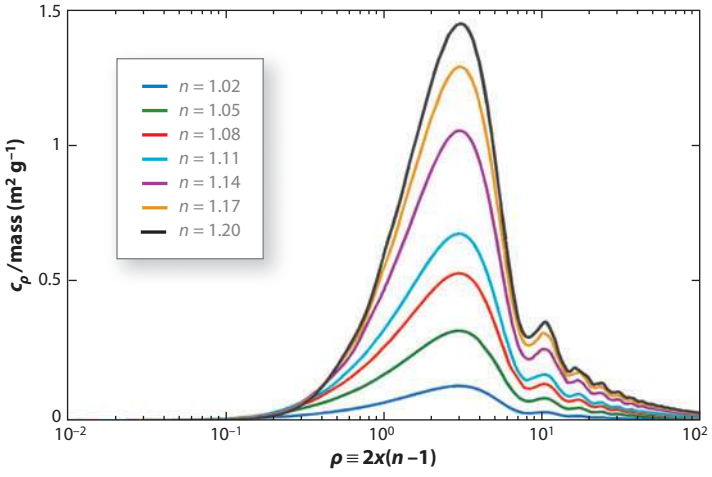

Figure 3

Particulate-mass-normalized beam attenuation as a function of $\rho \equiv 2x(n-1)$ for different values of the real part of the index of refraction, n ($n' = 0.0001$). Density of materials is assumed to follow $1{,}024[1 + 2.22(n-1)]$ kg m^{-3}, as suggested by Babin et al. (2003) for organic materials.

water fraction increases (ρ), one would predict that the size of maximal scattering per mass will increase with increasing water content of the aggregates (as its bulk index of refraction decreases, becoming closer to that of water). Indeed, when using a model developed to explain aggregates scattering (Boss et al. 2009a, Latimer 1985), the position of the maxima is observed to shift to larger sizes. Using the Gladstone-Dale relationship, the effective index of refraction of the aggregate can be computed from that of the particles of which it is composed: $(n-1)_{\text{aggregate}} = F(n-1)_{\text{particle}}$. Hence, the position of the maxima in the mass-normalized attenuation will be approximately at

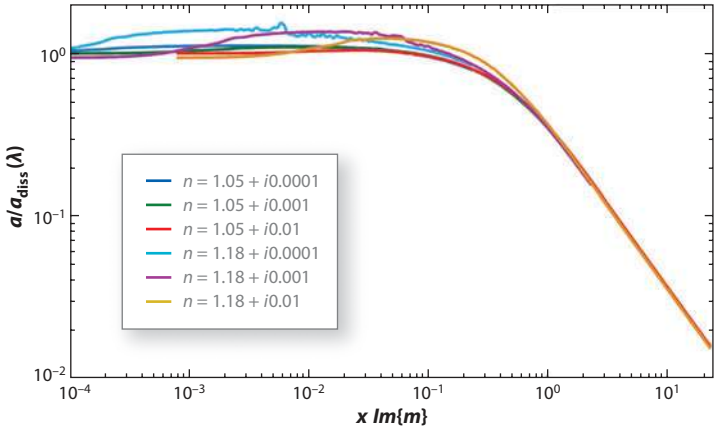

Figure 4

Particulate absorption normalized by the dissolved absorption ($4\pi n'/\lambda$) as a function of the product of the size parameter (x) and the imaginary part of the index of refraction ($n' = Im\{m\}$). The range of indices of refraction brackets the bulk of those of oceanic particles.

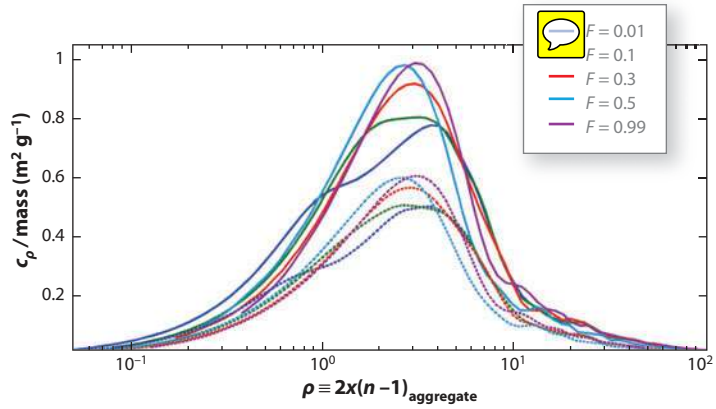

Figure 5

Particulate-mass-normalized beam attenuation as a function of $\rho \equiv 2x(n-1)_{aggregate}$ for particles differing in their index of refraction of their solid fraction ($m = 1.15 + 0.0001i$, *solid*; $m = 1.05 + 0.0001i$, *dashed*) and fluid fraction (*color*), using an optical model for aggregates based on work of Latimer (1985) and applied to marine aggregates by Boss et al. (2009a), with $\lambda_{vac} = 660$ nm. Density of inorganic (*solid*) and organic (*dashed*) materials are assumed to be 2,650 and 1,380 kg m^{-3}, respectively.

$x = 3F/[2(n_p - 1)]$ (consistent with **Figure 5**); for example, the size of the maximum for an aggregate with $F = 0.99$ (that is, 99% of its volume is water, or 1% solid fraction) is approximately 100 times that of an aggregate with 1% water fraction. Similarly, absorption by aggregate is now driven by $n'_{aggregate} = Fn'_{particle}$; thus, reduction to 50% of dissolved absorption occurs at $x \cdot n'_{aggregate} \sim 0.8$, e.g., for $d \sim 0.25\lambda/(Fn'_{particle})$ (consistent with results in **Figure 6**). It follows that the aggregation state of particles (e.g., their fluid fraction) and their size, in addition to the optical characteristics of the constituent particles, are the primary determinants of the optical properties of that aggregate.

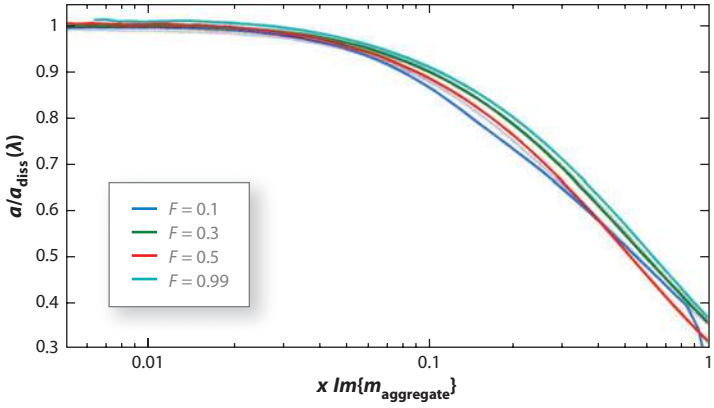

Figure 6

Particulate absorption (normalized by dissolved absorption) as a function of the product of the size parameter (x) and the imaginary part of the index of refraction ($n' = Im\{m_{aggregate}\}$), for particles differing in their index of refraction of their solid fraction ($m = 1.05 + 0.005i$, *solid*; $m = 1.05 + 0.001i$, *dashed*) and fluid fraction (*color*), using an optical model for aggregates based on work of Latimer (1985) and applied to marine aggregates by Boss et al. (2009a), with $\lambda_{vac} = 660$ nm.

Optical Methods to Obtain Information on Underlying Plankton and Particle Sizes: From Single Particle Properties to Bulk Optics to Imaging

There exist different approaches to measure size distribution of oceanic particles. Works summarizing existing methods include Syvitski (1991) and Xu (2000) as well as the recent reviews by Jonasz & Fournier (2007) and Benfield et al. (2007). Given that, we focus here on in situ optical techniques to obtain information regarding particulate size characteristics, limiting ourselves to commercial instruments and those to be commercialized shortly.

Size distribution characteristics inverted from bulk optical properties. There exist a variety of techniques to obtain information regarding the size distribution of a suspension of particles in a fluid, which have been applied to oceanographic measurements. As with all inverse methods, the inversion problem may be non-unique or very sensitive to noise; thus, assumptions regarding acceptable solutions as well as data regularization and conditioning are often applied (see ch. 6. in Shifrin 1988). Inversion of near-forward scattering has been used to create PSD for both in situ and laboratory suspension of particles from approximately 2 μm to 1 mm using such instruments as the in situ and laboratory LISST (e.g., Sequoia Scientific) (Agrawal & Pottsmith 2000). Smaller-sized particles can also be measured using larger angle dimensions in the volume-scattering function as measured with the laboratory instrument Heleos II (Wyatt & Jackson 1989) or using in situ data (Shifrin 1988, Zhang et al. 2011). Spectral beam attenuation of particles has been measured with commercial transmissometers, AC meters (WETLABS). The spectral characteristic has also been related to the size distribution [through inversions as in Volz (1954) and Van de Hulst (1981)] and found to agree with measurements based on the Coulter counter on a vessel or LISST in situ (Boss et al. 2001). Finally, the spectrum of backscattering inferred from remotely sensed ocean color has been linked to tendencies of the particulate size distribution in the ocean (Kostadinov et al. 2009, Loisel et al. 2006) as well as distributions of phytoplankton functional types (Alvain et al. 2008, Kostadinov et al. 2010) and inverted absorption spectra (Ciotti & Bricaud 2006).

Size distribution characteristics inverted from single particle optical properties. Flow cytometers perform automated enumeration of micron-sized particles (e.g., pico-phytoplankton) and estimation of their individual size based on side scattering, forward scattering, and the fluorescence characteristics of individual particles flowing through a laser beam (see the recent review by Yentsch & Yentsch 2008). This method has been used routinely in labs since the 1980s, and commercial instruments for in situ analysis exist [e.g., CytoBuoy (Dubelaar & Gerritzen 2000)]. Size range for these measurements is $0.5 < d < 10$ μm.

Size distribution characteristics obtained from optical imaging of particles. Imaging cytometers are instruments triggered by optical properties and take microscopic pictures of particles directed at a camera's focal plane (Olson & Sosik 2007, Sieracki et al. 1998). The size range for these measurements is $10 < d < 200$ μm. Silhouette cameras measuring light absorbance in different beams, such as the Laser Optical Particle Counter (LOPC, Brooke Ocean), are deployed on a variety of platforms to study zooplankton and particles, having 100 μm $< d <$ 1.5 mm (Checkley et al. 2008, Finlay et al. 2007, Herman & Harvey 2006, Herman et al. 2004, Vanderploeg & Roman 2006). Photographic and more recently CCD (charge-coupled device) cameras have been used to study aggregates and plankton, with sizes ranging from a few tens of micrometers $< d <$ to a few millimeters (Benfield et al. 2007, Davis et al. 1992, Davis et al. 2005, Gorsky et al. 1992a, Picheral et al. 2010, Ratmeyer & Wefer 1996). Several of these cameras are commercially

available [LOPC, UVP, Video Plankton Recorder (VPR)], most recently the holographic cameras detecting the volumetric abundance of particles (Graham & Smith 2010) spanning 20 μm < d < 7 mm (LISST-HOLO, Sequoia Scientific).

Differentiating Between Dead and Living Particles

Bulk optical measurements need to distinguish between plankton and other particles in the water column and get the composition of aggregates (mineral versus organic matter) or basic information on plankton taxa. For a pool of small particles (<100 μm), phytoplankton and detritus can be sorted by comparing bulk measurements at different wavelengths (Bricaud & Stramski 1990), whereas the ratio of backscattered to total scattered light provides a means for distinguishing the relative contributions of inorganic and organic particles (Twardowski et al. 2001).

For larger objects, imaging systems provide information on individual objects, which can be sorted for living plankton (Benfield et al. 2007). For example, plankton >500 μm such as crustacean (e.g., copepods and euphausiids) and gelatinous taxa or stages (e.g., medusae and tunicates or eggs and larvae) can be separated from particles of the same size range, which include aggregates, abandoned houses of larvaceans, mucous webs of pteropods, and associated material. Many of these other particles are fragile and are not retained and/or preserved by meshes of filters or nets (Gonzalez-Quiros & Checkley 2006). Therefore, the number and biomass contributions of the organisms versus the particles are not well known. Obtaining both size distributions and qualitative information in situ is still challenging, but progress has been made recently using various optical and imaging instruments. For example, during the BOUM cruise in the Mediterranean Sea (July 2008), the UVP was deployed on a longitudinal transect from the east to west basin during short-term stations and three sites were selected for their oligotrophic characteristics in the eastern (site C), central (site B), and western (site A) Mediterranean Sea (Moutin et al. 2011). Experts then performed manual image analysis and visual verification of the plankton (>500 μm) on the images as described by Stemmann et al. (2008b). Compared with nonliving particles, zooplankton organisms were rare at all sites. **Figure 7** shows the size spectra of radiolarians, crustaceans (mostly copepods), all other taxa pooled in one group, and all living organisms. The comparison between particles and zooplankton size spectra for the same size range (500 μm to a few millimeters) shows that the dominant zooplankton in abundance were radiolaria and, most striking, that living organisms were 1%–15% of the total particles detected by the UVP in the >500-μm size range. These ratios are slightly lower than those reported earlier for the OPC (25%) and LOPC (20% ± 14%) in the California Current system (Gonzalez-Quiros & Checkley 2006, Jackson & Checkley 2011). The differences in the reported proportions may be due to the trophic status of the ecosystems and the lower efficacy of the trophic change from small to large organisms in the oligotrophic Mediterranean systems. Future instruments should be able to better distinguish between plankton and aggregates.

Imaging techniques not only allow macrozooplankton to be identified, but also can reveal information on the nature and content of large particles. **Figure 8** shows several examples of different types of aggregates commonly found in the upper 200-m depth of Monterey Bay during July 2010 (GateKeeper cruise). Opaque cylindrical particles throughout the water column, long fibers in the upper 100-m depth, and aggregates most probably consisted of euphausiids fecal pellets (which were abundant in the nets; D.M. Checkley, personal communication), diatom chains, and aggregates constituted by different elements (including a sticky radiolarian). In the future, multispectral imaging and higher-definition images will allow for better identification of the organic and mineral constituents of aggregates.

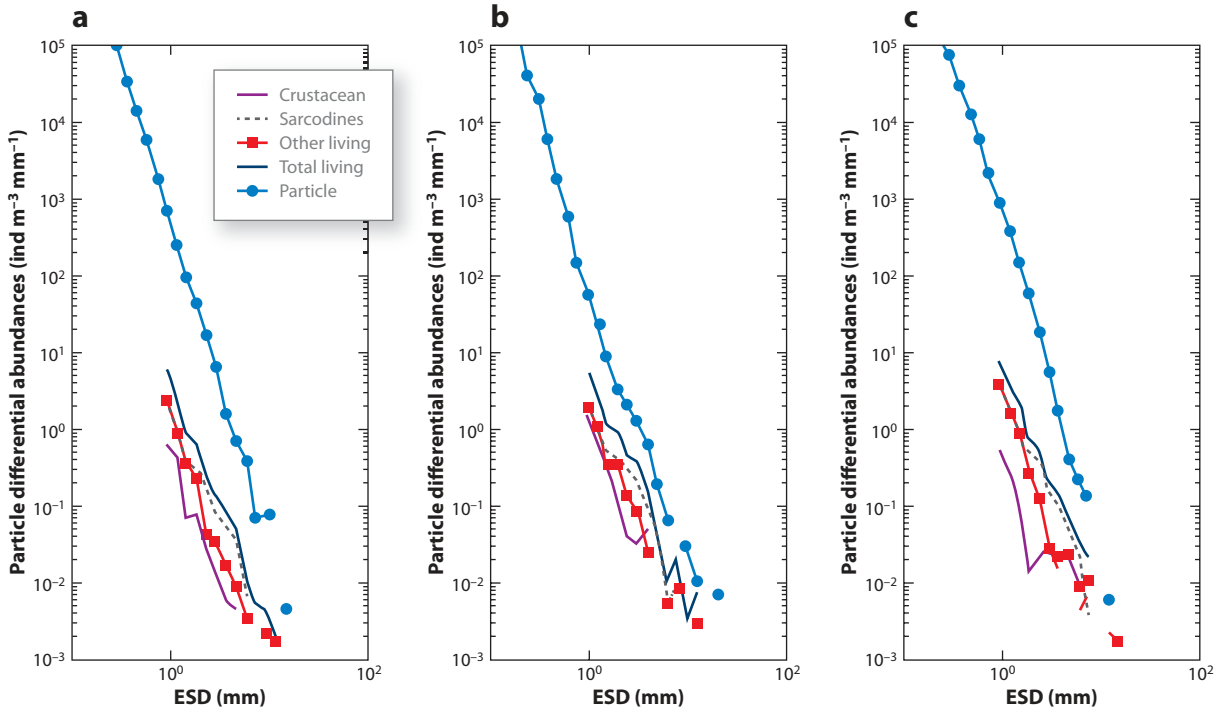

Figure 7

Particles and zooplankton differential abundances obtained by the Underwater Vision Profiler (Picheral et al. 2010) at three sites in the (*a*) eastern (site C), (*b*) central (site B), and (*c*) western (site A) Mediterranean Sea during the BOUM (Biogeochemistry from the Oligotrophic to the Ultra-Oligotrophic Mediterranean) cruise in July 2008. Particles were counted automatically from 60 μm in equivalent spherical diameter (ESD) and thus include nonliving particles and plankton organisms. The different taxa were counted manually on the images only for sizes >500 μm; at smaller sizes, taxa could not be identified.

SIZE EFFECTS ON THE FOOD WEB AND VERTICAL FLUXES

The size effect on light attenuation is secondary to concentration, but size is important in determining the flux of nutrient and light into phytoplankton cells and, hence, provides a physical constraint on their growth rate (Finkel & Irwin 2000, Karp-Boss et al. 1996). Available light for visual predators may affect trophic interactions in the sea, as it has been proposed as an explanation for the shift between zooplanktonivorous fishes and jellyfish in the northern European seas (Aksnes et al. 2004, Sornes & Aksnes 2004, Sornes & Aksnes 2006, Sornes et al. 2008). Therefore, measuring PSD and knowing the particle properties (see **Figure 5**) to infer light attenuation in the water column of different particle size classes may be helpful in understanding changes in the pelagic ecosystem. In addition, as size of the primary producers increases, the size of secondary producers and detritus increases, yielding a situation where vertical export becomes important (Boyd & Newton 1999, Guidi et al. 2008, Guidi et al. 2009). This aspect is developed in the following sections.

Global models have predicted that the strength of oceanic CO_2 sinks may already be decreasing, leading to a positive feedback on atmospheric CO_2 concentrations (Canadell et al. 2007). Unfortunately, it is clearly recognized in the oceanographic community that global models do not adequately represent observed biogenic particle fluxes to the deep ocean (Gehlen et al. 2006). As noted in the most recent review of the processes controlling the oceanic biological pump (Boyd & Trull 2007), "no models have yet incorporated sufficient complexity to capture the

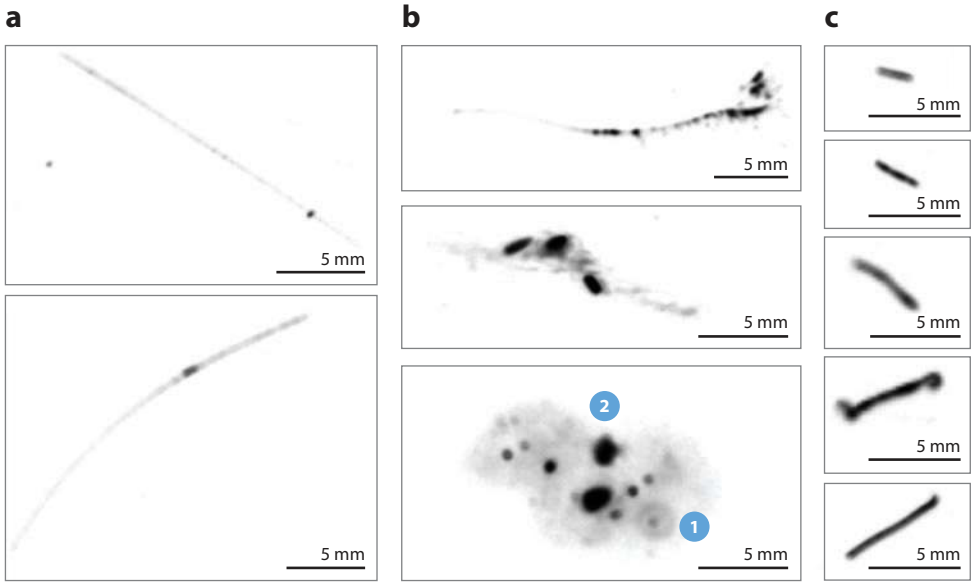

Figure 8

Examples of in situ images: (*a*) elongated particles, possibly diatom chains, from the upper 100-m depth; (*b*) different types of aggregates (①, radiolaria organism; ②, small opaque particles embedded in the aggregate matrix); (*c*) cylindrical particles possibly consisting of euphausiids fecal pellets.

observed variability of export fluxes." The reason is that we have not yet quantified the processes producing or transforming the particle vertical flux in the water column and the carbon budget is unbalanced (Burd et al. 2010). The most critical parameter for particle flux is the particle settling speed (Fasham et al. 1990). Particle size, packaging, and ballast are the key factors determining settling speed (McDonnell & Buesseler 2010, Stemmann et al. 2004b), but currently, only particle settling speed as a function of size can be almost routinely measured or assessed in the laboratory (Hansen et al. 1996, Iversen & Ploug 2010, Trent et al. 1978) or in situ by direct measurements (Alldredge & Gotschalk 1988) or using sediment traps (Guidi et al. 2008, McDonnell & Buesseler 2010). Various relationships have been found probably as a consequence not only of the various shapes for same-sized aggregates (**Figure 9*a***), but also of not taking into account the ballast effect of particles that have different mineral constituents.

Size can be used as a scaling factor and aggregation criterion to produce a macroscopic description of the pelagic ecosystems with the aim of improving the predictive capacity of global models in anticipation of future responses of oceanic ecosystems to climate change. Advances in optical sensors and imaging analysis tools have significantly increased our ability to measure sizes and abundances of organisms and particles in aquatic ecosystems. For example, size can also be used to obtain the specific growth rate of phytoplankton by analyzing time series of single cell size properties obtained with in situ flow cytometers (Sosik et al. 2003). Size-based mathematical models have also been developed for individual physiological and population change rates and for biomass flow between trophic levels. Broader spatial and longer temporal coverage of size spectra are expected in the coming decade, notably, those using autonomous drifters (Johnson et al. 2009) equipped with size-capturing sensors as has been successfully shown recently (Checkley et al. 2008).

Therefore, there is an urgent need for integrating field surveys, laboratory experiments, and models, in addition to developing methods for analyzing distributions and process rates of aquatic

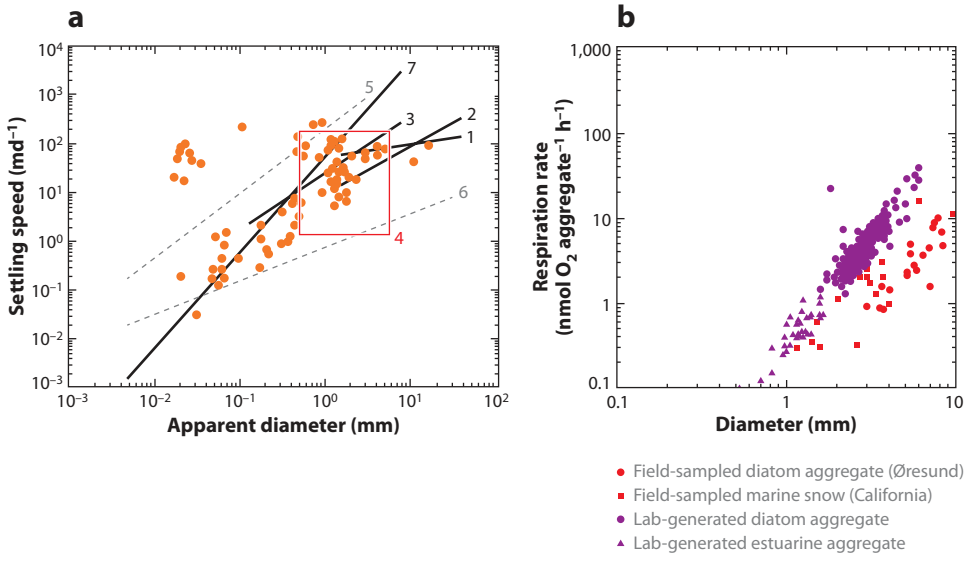

Figure 9

Allometric relationships between the size of aggregates and (*a*) aggregate settling speed (Stemmann et al. 2004b) and (*b*) measured respiration rates by colonial microbes in aggregates of different sources as a function of aggregate size (*symbols*) (modified from Ploug 2001). In panel *a*, different data points and regressions are used (for a full explanation, see Stemmann et al. 2004b).

organisms. More realistic models adding particle size spectra could be an alternative to the current biogeochemical models used to forecast global climate change. The following sections discuss the importance of size for aggregate remineralization by bacteria, zooplankton impact on the settling of aggregates, zooplankton ecophysiology scaling with size, and an integrating modeling framework.

Marine Particles Are Islands of Plenty for Microbes

Aggregates are sites of enhanced biological activity. Several studies have found that bacterial concentrations in aggregates are greater by a factor of up to 10^3 relative to the surrounding waters (Alldredge & Silver 1988, Davoll & Silver 1986, Grossart et al. 2003, Silver et al. 1998, Silver et al. 1978, Turley & Mackie 1994). Their abundance and their activity increase with aggregate size (Ploug & Grossart 2000, Ploug et al. 2008b). Protozoa are also important members of detrital communities, and they may feed on the bacteria (Caron et al. 1982, Kiørboe 2003, Silver & Gowing 1991, Silver et al. 1984). Attached bacteria metabolize and solubilize the particulate organic matter decomposing aggregates (Grossart & Simon 1998, Smith et al. 1992). Ploug (2001) has shown that respiration rate by bacteria on aggregates scales with their size (**Figure 9*b***). Direct metabolism and solubilization both represent losses to particle mass, but solubilization provides food for the free living bacteria and creates a chemical plume that fuels free bacteria with fresh dissolved organic matter and allows a particle to be detected by zooplankton (Kiørboe & Jackson 2001, Kiørboe et al. 2001).

Microbial consumption of particle mass can also affect particle geometry by hollowing out the particle or by shrinking it. In either case, it can change the mass-length relationship and, hence, the settling speeds. Biddanda & Pomeroy (1988) described a characteristic pattern of decomposition: growth of attached bacteria, aggregation of detritus, growth of protozoa feeding on bacteria, and

subsequent disaggregation. A similar pattern of microbial succession and particle alteration has been described for discarded larvacean houses (Davoll & Silver 1986) and tunicate feces (Pomeroy & Deibel 1980).

Size Is an Important Property for Interorganism and Particle-Organism Interactions

Size is also of great importance in terms of the manner in which organisms obtain contact for processes such as predation, grazing, mating, swarming, or aggregation (Jackson 1990, Jackson & Burd 1998, Jackson & Kiørboe 2004, Kiørboe 2001, Kriest & Evans 2000, Stemmann et al. 2004a). Encounter rates for inert particles in marine environments were first studied for inert particles by McCave (1983), who proposed a model to calculate the probability of an encounter between two particles as a function of their size and different processes occurring in the nepheloid layers: Brownian diffusion (negligible for $d > 1$ μm), differential sedimentation, and shear or turbulence. Later, Jackson (1990) used a model of the physical coagulation of growing a phytoplankton population to explain the end of the phytoplankton bloom by aggregation and subsequent settling out of the mixed layer.

From the perspective of global biogeochemical modeling, size is an attractive alternative, as the kernels for encounter rate (processes by which encounters occur) are all related to the size of particles (living or not). Yet, for zooplankton, the behavior is far more complex than a Brownian motion and is affected by many external factors (Schmitt & Seuront 2001, Schmitt et al. 2006). Several studies have started to study specific behavior: Jackson & Kiørboe (2004) provide a kernel formulation for the finding of particles in zooplankton, using a chemodetection of the chemical plume following particles in the marine environment. Such formulation is also related to the size of both zooplankton and particles. These mechanisms can be added to other grazing behaviors defined by Visser et al. (2001), e.g., ambush, cruising, or flux feeding (also related to size). The variety of swimming behaviors in zooplankton seems to be very large (Visser & Kiørboe 2006), but some simplifications can be used: For example, Baird & Suthers (2007) used the simple curvilinear model of Jackson (1995) to represent all the interactions between particles in a pelagic ecosystem. Currently, modeling studies are still scarce, and they have not been constrained with plankton or particle size spectra. Future instruments combining different sensors will provide more quantitative and qualitative data of the different players in the pelagic ecosystem (**Figure 10**) that will allow researchers to better constrain the diversity of mechanistical models for particle dynamics.

From Particle and Plankton Measures of Size to Conceptual and Mathematical Schemes of the Pelagic Ecosystem Role in the Biological Pump

The following section discusses the possible integration of PSD in biogeochemical models. In the past two decades, global ecosystem models used to quantify the strength of the biological pump have focused on creating a functional representation of mostly phytoplankton in the surface ocean (**Figure 11**). These box models divided the marine ecosystem into several dynamic compartments. The first models of marine ecosystems dynamics contained only one variable, the phytoplankton (Fleming 1939, Riley & Bumpus 1946). Soon after, models contained three variables, i.e., nutrient, phytoplankton, and zooplankton (Riley et al. 1949). The development of computers has allowed the number of variables to increase to seven (Fasham et al. 1990). The box models became a standard for the subsequent development of biogeochemical models. Current biogeochemical models have more than 11 compartments (Aumont et al. 2003, Le Quere et al. 2005), and recent modeling frameworks simulate a great number of phytoplankton types from which emerging communities can be simulated (Follows et al. 2007).

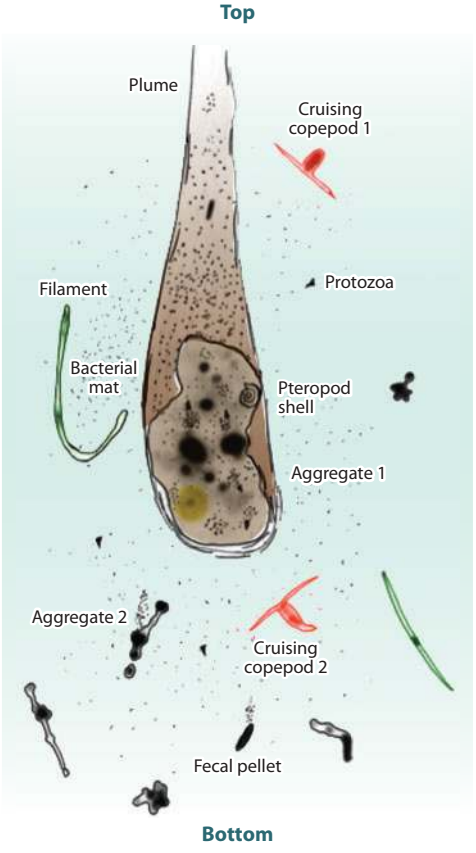

Figure 10

A view of a settling aggregate in the ocean based on an idealized multisensor instrument. Such an instrument should sense the aggregate's effects on its environment, such as chemical plumes left behind the settling aggregate; identify particle shapes; and differentiate constituents [e.g., organic (fecal pellet) and mineral (pteropod shell) embedded in the aggregate]. The same instrument should detect basic components of the microbial community (free and attached bacteria, larger protozoa) and the metazoa feeding and transforming the settling aggregate. Cruising copepod 1 is attracted by the dissolved organic plume, whereas cruising copepod 2 is attracted by hydromechanical disturbance in front of the aggregate. Filaments may be phytoplankton chains. Note that all objects have been redrawn from original images generated by the Underwater Vision Profiler in Monterey Bay, California. The large aggregate is also shown in **Figure 8**.

Previous biogeochemical models lacked the description of processes carried out by zooplankton organisms because of the complexity of this group and the small and diverse number of data sets (Buitenhuis et al. 2006). Zooplankton have often been represented as a closure variable with fixed rates in compartment models, although their interactions with phytoplankton may be important to understand the ecosystem dynamics. However, more structured models differentiating between sizes, ages, and/or stages have been developed to describe zooplankton population demographics (Carlotti & Sciandra 1989, Carlotti & Wolf 1998, Hofmann & Ambler 1988). However, population dynamics models may often be too complicated for global scales because the population dynamic has to be known in detail and modeling population dynamics of numerous species is challenging. Hence, most models of marine ecosystems rely on functional group partitioning and use fixed predation rates between few zooplankton groups.

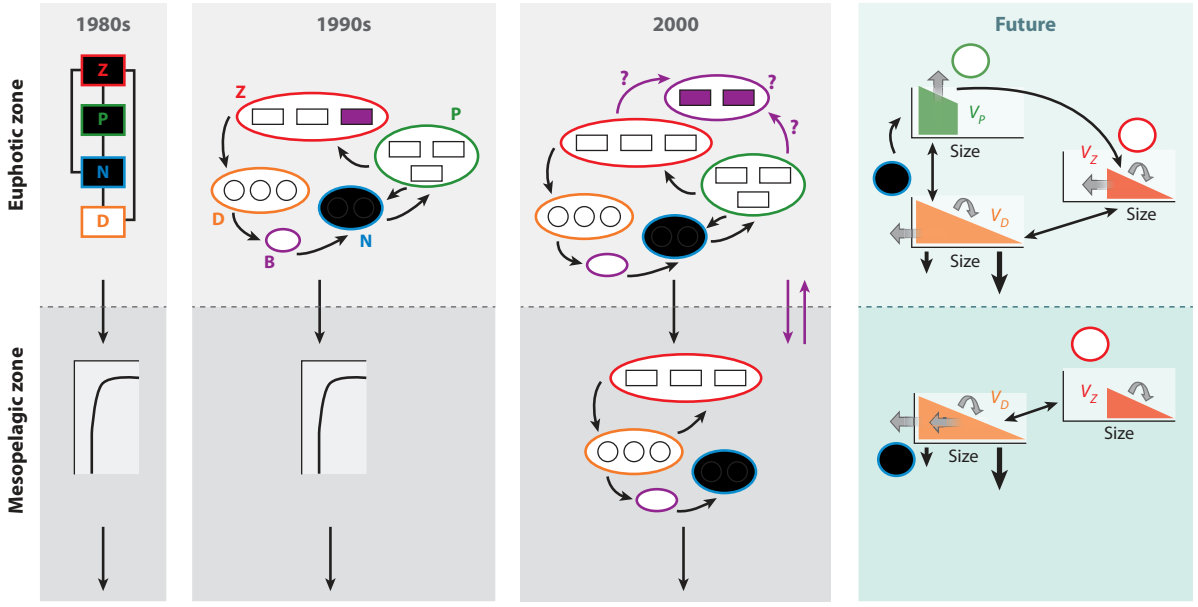

Figure 11

Scheme showing the evolution of the conceptual framework for biochemical modeling since the 1980s. Living organisms (plankton) are represented by rectangles, whereas nutrients and detritus are indicated by circles. Arrows represent the flow of mass from one compartment to the other. Ellipses are drawn to show that each ecosystem trophic level can contain more than one compartment. The complexity of the models has increased over time by adding more compartments and including higher trophic levels. In the future, some functional groups may be replaced by a size-based description of the organisms and detritus. All compartments may not be described with size because they are too specific. This is particularly true for the phytoplankton because either they do not prey on each other or they have very specific functions (N_2 fixators, calcifiers) and several zooplankton taxa (tunicates, jellyfish). Crustaceans may be good candidates for a size-based description because they share many metabolic pathways and lifecycle dynamics. The proposed model should be simple enough to be included in three-dimensional biogeochemical models. Abbreviations: N, nutrients; P, phytoplankton; Z, zooplankton; D, detritus; B, microbial loop; V_P, volume spectrum of phytoplankton; V_Z, volume spectrum of zooplankton; V_D, volume spectrum of detritus.

Very recently, several models have included size-based physical and biological interactions, even in the mesopelagic zone. Those models are based on a fundamental assumption that size is a structuring dimension of ecological systems along which dynamics can be projected. Taking such an approach has been recently proposed, but the models to date have not been tested with data (Baird et al. 2004, Maury et al. 2007). The reason for using scaling with size for physiological rates is that the rates scale more with size than with taxonomy (Fenchel 1974, Glazier 2005, Legendre & Michaud 1998, Von Bertalanffy 1957, West et al. 2003). Scaling with size is used for encounter rates between zooplankton organisms and detritus because predator-prey interactions and particle-particle encounter rates are believed to scale with size (Hansen et al. 1997; Jackson 1993, 2005; Jackson & Burd 1998; Jackson & Kiørboe 2004; Kiørboe 2000, 2001, 2008; Kiørboe & MacKenzie 1995; Kiørboe & Thygesen 2001; Kiørboe & Titelman 1998; Kiørboe & Visser 1999). Finally, for particle-particle interactions, numerous size-based models have been proposed with different levels of complexity (Jackson 1990, Kriest & Evans 1999, Riebessel & Wolf-Gladrow 1992). Recent models include explicit formulations of particle size and mass with 2D size spectra (Jackson 2001) or with simpler representation in global models (Gehlen et al. 2006). Therefore, these mechanistic models for interactions within the biological groups could be used for relevant compartments in the upper layer of future ecosystem models (**Figure 11**).

For more than two decades, research in oceanography has focused on the role and functioning of the upper 200-m layers of the ocean. The deeper ocean was regarded as a black box because of the lack of data. Despite recent advances in modeling of surface ocean ecosystem processes at the global scale (Aumont & Bopp 2006, Le Quere et al. 2005, Moore et al. 2004), the description of particle fluxes in global ocean biogeochemical models still mostly relies on exponential or power-law functions (Armstrong et al. 2002, Betzer et al. 1984, Martin et al. 1987, Suess 1980). Yet, marine particle fluxes and their attenuation with depth display strong regional and temporal variability in response to production regimes and their seasonality (Berelson 2001, Boyd & Trull 2007, Lutz et al. 2002). The relationship between surface ocean ecosystem structure and variability is not captured by these simplified approaches.

The model by Kriest & Evans (2000) provides an interesting alternative suitable for global-scale applications. It relies on the explicit parameterization of particle interactions (aggregation/disaggregation). Particle number and size are the stated variables. The particle sinking speed is computed as a function of PSD. This model was implemented in the French biogeochemical model PISCES and compared with other particle flux parameterizations of varying complexity (Gehlen et al. 2006). However, the approach by Kriest & Evans (2000) still relies on simplifying assumptions that were not tested within the framework of PISCES in terms of their consequences for the prediction of particle dynamics (mass flux, sinking speed, temporal and spatial variability). For instance, the description of the particle size spectrum by a constant exponent contradicts observations reporting variability with depth of the latter (Guidi et al. 2009, Iversen et al. 2010). This variability most likely reflects the impact of zooplankton feeding and microbial degradation on particle size spectra. Different mesopelagic communities are expected to differentially alter particle fluxes in terms of mass and size distribution as was suggested by the model of Stemmann et al. (2004b). Here also, measuring PSD would lead to general improvements in the description and dynamics of zooplankton and dead particle models in the mesopelagic layers (**Figure 11**).

A VISION FOR THE FUTURE

Appropriate temporal and spatial scales of marine production can be studied using satellite data for the surface of the ocean, and now, underwater autonomous profiling floats and gliders have been developed to study deeper layers. The international ARGO project, which currently has an array of approximately 3,000 profiling floats deployed in the world's oceans, has proven to be an invaluable tool in modern physical oceanography. It provides, on a routine basis and with great detail, the heat and salt content of the upper ocean and is used to constrain circulation models. As price is reduced and the variety of instrumentation measuring ecological parameters is increased, there is hope of using a similar observational system to constrain biogeochemical models (Claustre et al. 2010, Johnson et al. 2009). Incorporation of instrumentation capable of differentiating individual size, functional groups, as well as species could provide data to map more complex ecosystems. Such an array of profiling floats will revolutionize our ability to understand the fate and distribution of organic matter in the oceans.

SUMMARY POINTS

1. In the open ocean, the first building blocks of organic particles are produced through different pathways among which primary production in the euphotic zone is the most important. Sedimentation of these particles in the deep ocean constitutes one aspect of the biological pump whose strength can affect global climate.

2. PSDs are indicators of pelagic ecosystem trophic states and functioning. Their shapes can indicate the importance of biological and physical processes (trophic flows, aggregation, disaggregation) that transform the organic matter produced at the surface. Assuming that particle settling speed is mainly related to size, they can be used to calculate vertical flux of elements to the deep sea. This assumption is a first-order simplification because particle composition is also critical to assess the settling speed.
3. PSDs can be calculated in their full size range (a few micrometers to centimeters) using optical properties measured by different instruments. These instruments can measure individual and bulk properties such as size, nature (living or dead), and basic information on constituting elements (for example, calcite). Future technological developments should point toward better measurement of mineral versus organic content of particles and the fluid fraction of aggregates. This knowledge and the development of mathematical frameworks are critical to correctly estimate particle settling speed and element vertical fluxes.
4. Within the next 10 years, these instruments will be tested on Lagrangian autonomous vehicles to gather plankton and particle size spectra remotely and deep in the ocean. Successful deployment of these instruments and the delivery of large amounts of data could lead to a revolution in biogeochemical oceanography.
5. Such data on PSD and particle composition can be used to constrain biogeochemical models to better understand biological pump processes and quantify their strength synoptically.

DISCLOSURE STATEMENT

The UVP and ZooScan instruments were originally developed in L.S.'s lab, although he has had no subsequent financial or commercial relationships with them.

ACKNOWLEDGMENTS

The authors thank the many colleagues who through discussions and collaborations have helped us to develop our knowledge on plankton and particle dynamics as detected using their optical properties. It was also substantially improved based on the critical comments provided by Louis Legendre and George Jackson. UVP data were obtained during the BIOSOPE and BOUM cruises with support from the French national LEFE-CYBER program and during the U.S. NSF-supported Gatekeeper program (OCE-0928425). L.S. was supported by funding from the seventh European Framework Program (JERICO). Support to E.B. was provided by NASA's Ocean Biology and Biogeochemistry program.

LITERATURE CITED

Aas E. 1996. Refractive index of phytoplankton derived from its metabolite composition. *J. Plankton Res.* 18:2223–49

Agrawal YC, Pottsmith HC. 2000. Instruments for particle size and settling velocity observations in sediment transport. *Mar. Geol.* 168:89–114

Aksnes DL, Nejstgaard J, Soedberg E, Sornes T. 2004. Optical control of fish and zooplankton populations. *Limnol. Oceanogr.* 49:233–38

Alldredge A. 1998. The carbon, nitrogen and mass content of marine snow as a function of aggregate size. *Deep-Sea Res. Part I* 45:529–41

Alldredge AL. 2000. Interstitial dissolved organic carbon (DOC) concentrations within sinking marine aggregates and their potential contribution to carbon flux. *Limnol. Oceanogr.* 45:1245–53

Alldredge AL, Gotschalk C. 1988. In situ settling behavior of marine snow. *Limnol. Oceanogr.* 33:339–51

Alldredge AL, Passow U, Logan BE. 1993. The abundance and significance of a class of large, transparent organic particles in the ocean. *Deep-Sea Res. Part I* 40:1131–40

Alldredge AL, Silver MW. 1988. Characteristics, dynamics and significance of marine snow. *Prog. Oceanogr.* 20:41–82

Alvain S, Moulin C, Dandonneau Y, Loisel H. 2008. Seasonal distribution and succession of dominant phytoplankton groups in the global ocean: a satellite view. *Glob. Biogeochem. Cycles* 22:GB3001

Armstrong RA, Lee C, Hedges JI, Honjo S, Wakeham SG. 2002. A new, mechanistic model for organic carbon fluxes in the ocean based on the quantitative association of POC with ballast minerals. *Deep-Sea Res. Part II* 49:219–36

Aumont O, Bopp L. 2006. Globalizing results from ocean in situ iron fertilization studies. *Glob. Biogeochem. Cycles* 20:GB2017

Aumont O, Maier-Reimer E, Blain S, Monfray P. 2003. An ecosystem model of the global ocean including Fe, Si, P colimitations. *Glob. Biogeochem. Cycles* 17:GB1060

Babin M, Morel A, Fournier-Sicre V, Fell F, Stramski D. 2003. Light scattering properties of marine particles in coastal and open ocean waters as related to the particle mass concentration. *Limnol. Oceanogr.* 48:843–59

Baird ME, Oke PR, Suthers IM, Middleton JH. 2004. A plankton population model with biomechanical descriptions of biological processes in an idealised 2D ocean basin. *J. Mar. Syst.* 50:199–222

Baird ME, Suthers IM. 2007. A size-resolved pelagic ecosystem model. *Ecol. Model.* 203:185–203

Beaulieu SE, Mullin MM, Tang VT, Pyne SM, King AL, Twining BS. 1999. Using an optical plankton counter to determine the size distributions of preserved zooplankton samples. *J. Plankton Res.* 21:1939–56

Benfield MC, Grosjean P, Culverhouse PF, Irigoien X, Sieracki ME, et al. 2007. RAPID: research on automated plankton identification. *Oceanography* 20:172–87

Berelson WM. 2001. The flux of particulate organic carbon into the ocean interior: a comparison of four U.S. JGOFS regional studies. *Oceanography* 14:59–67

Betzer PR, Showers WJ, Laws EA, Winn CD, Ditullio GR, Kroopnick PM. 1984. Primary productivity and particle fluxes on a transect of the equator at 153°W in the Pacific Ocean. *Deep-Sea Res. Part I* 31:1–11

Biddanda BA, Pomeroy LR. 1988. Microbial aggregation and degradation of phytoplankton-derived detritus in seawater. 1. Microbial succession. *Mar. Ecol. Prog. Ser.* 42:79–88

Boss E, Pegau W, Gardner W, Zaneveld J, Barnard A, et al. 2001. Spectral particulate attenuation and particle size distribution in the bottom boundary layer of a continental shelf. *J. Geophys. Res.* 106:9509–16

Boss E, Slade W, Hill P. 2009a. Effect of particulate aggregation in aquatic environments on the beam attenuation and its utility as a proxy for particulate mass. *Opt. Express* 17:9408–20

Boss E, Taylor L, Gilbert S, Gundersen K, Hawley N, et al. 2009b. Comparison of inherent optical properties as a surrogate for particulate matter concentration in coastal waters. *Limnol. Oceanogr. Methods* 7:803–10

Boyd PW, Newton PP. 1999. Does planktonic community structure determine downward particulate organic carbon flux in different oceanic provinces? *Deep-Sea Res. Part I* 46:63–91

Boyd PW, Trull TW. 2007. Understanding the export of biogenic particles in oceanic waters: Is there consensus? *Prog. Oceanogr.* 72:276–312

Bricaud A, Stramski D. 1990. Spectral absorption coefficients of living phytoplankton and nonalgal biogenous matter: a comparison between the Peru upwelling area and the Sargasso Sea. *Limnol. Oceanogr.* 35:562–82

Brown JH, Gillooly JF, Allen AP, Savage VM, West GB. 2004. Toward a metabolic theory of ecology. *Ecology* 85:1771–89

Brun-Cottan JC. 1971. Etude de la granulométrie des particules marines, mesures effectuées avec un compteur Coulter. *Cah. Océanogr.* 23:193–205

Buitenhuis E, Le Quere C, Aumont O, Beaugrand G, Bunker A, et al. 2006. Biogeochemical fluxes through mesozooplankton. *Glob. Biogeochem. Cycles* 20:GB2003

Burd AB, Hansell DA, Steinberg DK, Anderson TR, Aristegui J, et al. 2010. Assessing the apparent imbalance between geochemical and biochemical indicators of meso- and bathypelagic biological activity: What the @$#! is wrong with present calculations of carbon budgets? *Deep-Sea Res. Part II* 57:1557–71

Burd AB, Jackson GA. 2009. Particle aggregation. *Annu. Rev. Mar. Sci.* 1:65–90

Canadell JG, Kirschbaum MUF, Kurz WA, Sanz MJ, Schlamadinger B, Yamagata Y. 2007. Factoring out natural and indirect human effects on terrestrial carbon sources and sinks. *Environ. Sci. Policy* 10:370–84

Carlotti F, Sciandra A. 1989. Population dynamics model of Euterpina acutifrons (Copepoda: Harpacticoida) coupling individual growth and larval development. *Mar. Ecol. Prog. Ser.* 56:225–42

Carlotti F, Wolf KU. 1998. A Lagrangian ensemble model of Calanus finmarchicus coupled with a 1-D ecosystem model. *Fish. Oceanogr.* 7:191–204

Caron DA, Davis PG, Madin LP, Sieburth JMN. 1982. Heterotrophic bacteria and bacterivorous protozoa in oceanic macroaggregates. *Science* 218:795–97

Checkley DM, Davis RE, Herman AW, Jackson GA, Beanlands B, Regier LA. 2008. Assessing plankton and other particles in situ with the SOLOPC. *Limnol. Oceanogr.* 53:2123–36

Ciotti AM, Bricaud A. 2006. Retrievals of a size parameter for phytoplankton and spectral light absorption by colored detrital matter from water-leaving radiances at SeaWiFS channels in a continental shelf region off Brazil. *Limnol. Oceanogr. Methods* 4:237–53

Claustre H, Antoine D, Boehme L, Boss E, D'Ortenzio F, et al. 2010. Guidelines towards an integrated ocean observation system for ecosystems and biogeochemical cycles. *Proc. OceanObs'09: Sustain. Ocean Obs. Inf. Soc.* (*Vol. 1*), Venice, Italy, Sept. 21–25, ESA Publ. WPP-306

Clavano WR, Boss E, Karp-Boss L. 2007. Inherent optical properties of non-spherical marine-like particles—from theory to observation. *Oceanogr. Mar. Biol.* 45:1–38

Cronin TW, Shashar N, Caldwell RL, Marshall J, Cheroske AG, Chiou TH. 2003. Polarization vision and its role in biological signaling. *Integr. Comp. Biol.* 43:549–58

Davis CS, Gallager SM, Solow AR. 1992. Microaggregation of oceanic plankton observed by towed video microscopy. *Science* 257:230–32

Davis CS, Thwaites FT, Gallager SM, Hu Q. 2005. A three-axis fast-tow digital Video Plankton Recorder for rapid surveys of plankton taxa and hydrography. *Limnol. Oceanogr. Methods* 3:59–74

Davoll PJ, Silver MW. 1986. Marine snow aggregates—life-history sequence and microbial community of abandoned larvacean houses from Monterey Bay, California. *Mar. Ecol. Prog. Ser.* 33:111–20

Dubelaar GBJ, Gerritzen PL. 2000. CytoBuoy: a step forward towards using flow cytometry in operational oceanography. *Sci. Mar.* 64:255–65

Duysens LNM. 1956. The flattening of the absorption spectrum of suspensions, as compared to that of solutions. *Biochim. Biophys. Acta* 19:1–12

Fasham MJR, Duclow HW, Mckelvie SM. 1990. A nitrogen-based model of plankton dynamics in the oceanic mixed layer. *J. Mar. Res.* 48:591–639

Fenchel T. 1974. Intrinsic rate of natural increase: the relationship with body size. *Oecologia* 14:317–26

Finkel ZV, Irwin AJ. 2000. Modeling size-dependent photosynthesis: light absorption and the allometric rule. *J. Theor. Biol.* 204:361–69

Finlay K, Beisner BE, Barnett AJD. 2007. The use of the Laser Optical Plankton Counter to measure zooplankton size, abundance, and biomass in small freshwater lakes. *Limnol. Oceanogr. Methods* 5:41–49

Fleming RH. 1939. The control of diatom populations by grazing. *J. Cons. Int. Explor. Mer* 14:210–27

Follows MJ, Dutkiewicz S, Grant S, Chisholm SW. 2007. Emergent biogeography of microbial communities in a model ocean. *Science* 315:1843–46

Gaedke U. 1992. The size distribution of plankton biomass in a large lake and its seasonal variability. *Limnol. Oceanogr.* 37:1202–20

Gallienne CP, Robins DB. 1998. Trans-oceanic characterization of zooplankton community size structure using an optical plankton counter. *Fish. Oceanogr.* 7:147–58

Gallienne CP, Robins DB, Woodd-Walker RS. 2001. Abundance, distribution and size structure of zooplankton along a 20° west meridional transect of the northeast Atlantic Ocean in July. *Deep-Sea Res. Part I* 48:925–49

Gardner WD, Richardson MJ, Carlson CA, Hansell D, Mishonov AV. 2003. Determining true particulate organic carbon: bottles, pumps and methodologies. *Deep-Sea Res. Part II* 50:655–74

Gehlen M, Bopp L, Ernprin N, Aumont O, Heinze C, Raguencau O. 2006. Reconciling surface ocean productivity, export fluxes and sediment composition in a global biogeochemical ocean model. *Biogeosciences* 3:521–37

Gillooly JF. 2000. Effect of body size and temperature on generation time in zooplankton. *J. Plankton Res.* 22:241–51

Gillooly JF, Brown JH, West GB, Savage VM, Charnov EL. 2001. Effects of size and temperature on metabolic rate. *Science* 293:2248–51

Gillooly JF, Charnov EL, West GB, Savage VM, Brown JH. 2002. Effects of size and temperature on developmental time. *Nature* 417:70–73

Glazier DS. 2005. Beyond the "3/4-power law": variation in the intra- and interspecific scaling of metabolic rate in animals. *Biol. Rev.* 80:611–62

Gonzalez-Quiros R, Checkley DM. 2006. Occurrence of fragile particles inferred from optical plankton counters used in situ and to analyze net samples collected simultaneously. *J. Geophys. Res.* 111:C05206

Gorsky G, Aldorf C, Kage M, Picheral M, Garcia Y, Favole J. 1992a. *Vertical distribution of suspended aggregates determined by a new underwater video profiler*. Presented at Coll. Prog. Natl. Determinisme Recrut., 3rd, Nantes, France

Gorsky G, Aldorf C, Kage M, Picheral M, Garcia Y, Favole J. 1992b. Vertical distribution of suspended aggregates determined by a new underwater video profiler. *Ann. Inst. Océanogr.* 68:275–80

Gorsky G, Ohman MD, Picheral M, Gasparini S, Stemmann L, et al. 2010. Digital zooplankton image analysis using the ZooScan integrated system. *J. Plankton Res.* 32:285–303

Graham GW, Smith W. 2010. The application of holography to the analysis of size and settling velocity of suspended cohesive sediments. *Limnol. Oceanogr. Methods* 8:1–15

Grossart HP, Kiørboe T, Tang K, Ploug H. 2003. Bacterial colonization of particles: growth and interactions. *Appl. Environ. Microbiol.* 69:3500–9

Grossart HP, Simon M. 1998. Bacterial colonization and microbial decomposition of limnetic organic aggregates (lake snow). *Aquat. Microb. Ecol.* 15:127–40

Guidi L, Jackson GA, Stemmann L, Miquel J, Picheral M, Gorsky G. 2008. Relationship between particle size distribution and flux in the mesopelagic zone. *Deep-Sea Res. Part I* 55:1364–74

Guidi L, Stemmann L, Jackson GA, Ibanez F, Claustre H, et al. 2009. Effects of phytoplankton community on production, size and export of large aggregates: a world-ocean analysis. *Limnol. Oceanogr.* 54:1951–63

Hansen JLS, Kiørboe T, Alldredge AL. 1996. Marine snow derived from abandoned larvacean houses: Sinking rates, particle content and mechanisms of aggregate formation. *Mar. Ecol. Prog. Ser.* 141:205–15

Hansen PJ, Bjornsen PK, Hansen BW. 1997. Zooplankton grazing and growth: scaling within the 2–2,000-μm body size range. *Limnol. Oceanogr.* 42:687–704

Harris RP, Wiebe PH, Lenz J, Skjoldal HR, Huntley M, eds. 2000. *ICES Zooplankton Methodology Manual*. San Diego: Academic. 684 pp.

Herman AW. 1992. Design and calibration of a new optical plankton counter capable of sizing small zooplankton. *Deep-Sea Res. Part I* 39:395–415

Herman AW, Beanlands B, Phillips EF. 2004. The next generation of Optical Plankton Counter: the Laser-OPC. *J. Plankton Res.* 26:1135–45

Herman AW, Harvey M. 2006. Application of normalized biomass size spectra to laser optical plankton counter net intercomparisons of zooplankton distributions. *J. Geophys. Res. Oceans* 111:C05S05

Hill PS, Boss E, Newgard JP, Law BA, Milligan TG. 2011. Observations of the sensitivity of beam attenuation to particle size in a coastal bottom boundary layer. *J. Geophys. Res. Oceans* 116:C02023

Hofmann EE, Ambler JW. 1988. Plankton dynamics on the outer southeastern U.S. Continental Shelf. Part II: a time-dependent biological model. *J. Mar. Res.* 46:883–917

Huntley ME, Zhou M, Nordhausen W. 1995. Mesoscale distribution of zooplankton in the California Current in late spring, observed by optical plankton counter. *J. Mar. Res.* 53:647–74

Iversen MH, Nowald N, Ploug H, Jackson GA, Fischer G. 2010. High resolution profiles of vertical particulate organic matter export off Cape Blanc, Mauritania: degradation processes and ballasting effects. *Deep-Sea Res. Part I* 57:771–84

Iversen MH, Ploug H. 2010. Ballast minerals and the sinking carbon flux in the ocean: carbon-specific respiration rates and sinking velocity of marine snow aggregates. *Biogeosciences* 7:2613–24

Jackson GA. 1990. A model of the formation of marine algal flocs by physical coagulation processes. *Deep-Sea Res. Part I* 37:1197–211

Jackson GA. 1993. Flux feeding as a mechanism for zooplankton grazing and its implications for vertical particulate flux. *Limnol. Oceanogr.* 38:1328–31

Jackson GA. 1995. Comparing observed changes in particle size spectra with those predicted using coagulation theory. *Deep-Sea Res. Part II* 42:159–84

Jackson GA. 2001. Effect of coagulation on a model planktonic food web. *Deep-Sea Res. Part I* 48:95–123

Jackson GA. 2005. Coagulation theory and models of oceanic plankton aggregation. In *Flocculation in Natural and Engineered Environmental Systems*, ed. I Droppo, G Leppard, S Liss, T Milligan, pp. 271–92. Boca Raton, FL: CRC

Jackson GA, Burd AB. 1998. Aggregation in the marine environment. *Environ. Sci. Technol.* 32:2805–14

Jackson GA, Checkley DM. 2011. Particle size distributions in the upper 100-m water column and their implications for animal feeding in the plankton. *Deep-Sea Res. Part I* 58:283–97

Jackson GA, Kiørboe T. 2004. Zooplankton use of chemodetection to find and eat particles. *Mar. Ecol. Prog. Ser.* 269:153–62

Jackson GA, Logan BE, Alldredge AL, Dam HG. 1995. Combining particle-size spectra from a mesocosm experiment measured using photographic and aperture impedance (Coulter and Elzone) techniques. *Deep-Sea Res. Part II* 42:139–57

Jackson GA, Maffione R, Costello DK, Alldredge AL, Logan BE, Dam HG. 1997. Particle size spectra between 1 μm and 1 cm at Monterey Bay determined using multiple instruments. *Deep-Sea Res. Part I* 44:1739–67

Jennings S, De Oliveira JAA, Warr KJ. 2007. Measurement of body size and abundance in tests of macroecological and food web theory. *J. Anim. Ecol.* 76:72–82

Jennings S, Warr KJ. 2003. Smaller predator-prey body size ratios in longer food chains. *Proc. R. Soc. Lond. Ser. B* 270:1413–17

Johnson KS, Berelson WM, Boss ES, Chase Z, Claustre H, et al. 2009. Observing biogeochemical cycles at global scales with profiling floats and gliders: prospects for a global array. *Oceanography* 22:216–25

Jonasz M, Fournier G. 2007. *Light Scattering by Particles in Water: Theoretical and Experimental Foundations*. Amsterdam: Elsevier Sci. 704 pp.

Karp-Boss L, Boss E, Jumars PA. 1996. Nutrient fluxes to planktonic osmotrophs in the presence of fluid motion. *Oceanogr. Mar. Biol. Annu. Rev.* 34:71–107

Kiørboe T. 2000. Colonization of marine snow aggregates by invertebrate zooplankton: abundance, scaling, and possible role. *Limnol. Oceanogr.* 45:479–84

Kiørboe T. 2001. Formation and fate of marine snow: small-scale processes with large-scale implications. *Sci. Mar.* 65:57–71

Kiørboe T. 2003. Marine snow microbial communities: scaling of abundances with aggregate size. *Aquat. Microb. Ecol.* 33:67–75

Kiørboe T. 2008. *A Mechanistic Approach to Plankton Ecology*. Princeton, NJ: Princeton Univ. Press

Kiørboe T, Grossart HP, Ploug H, Tang K. 2002. Mechanisms and rates of bacterial colonization of sinking aggregates. *Appl. Environ. Microbiol.* 68:3996–4006

Kiørboe T, Grossart HP, Ploug H, Tang K, Auer B. 2004. Particle-associated flagellates: swimming patterns, colonization rates, and grazing on attached bacteria. *Aquat. Microb. Ecol.* 35:141–52

Kiørboe T, Jackson GA. 2001. Marine snow, organic solute plumes, and optimal chemosensory behavior of bacteria. *Limnol. Oceanogr.* 46:1309–18

Kiørboe T, MacKenzie B. 1995. Turbulence-enhanced prey encounter rates in larval fish: effects of spatial scale, larval behaviour and size. *J. Plankton Res.* 17:2319–31

Kiørboe T, Ploug H, Thygesen UH. 2001. Fluid motion and solute distribution around sinking aggregates. I. Small-scale fluxes and heterogeneity of nutrients in the pelagic environment. *Mar. Ecol. Prog. Ser.* 211:1–13

Kiørboe T, Thygesen UH. 2001. Fluid motion and solute distribution around sinking aggregates. II. Implications for remote detection by colonizing zooplankters. *Mar. Ecol. Prog. Ser.* 211:15–25

Kiørboe T, Titelman J. 1998. Feeding, prey selection and prey encounter mechanisms in the heterotrophic dinoflagellate *Noctiluca scintillans*. *J. Plankton Res.* 20:1615–36

Kiørboe T, Visser AW. 1999. Predator and prey perception in copepods due to hydromechanical signals. *Mar. Ecol. Prog. Ser.* 179:81–95

Kostadinov TS, Siegel DA, Maritorena S. 2009. Retrieval of the particle size distribution from satellite ocean color observations. *J. Geophys. Res. Oceans* 114:C09015

Kostadinov TS, Siegel DA, Maritorena S. 2010. Global variability of phytoplankton functional types from space: assessment via the particle size distribution. *Biogeosciences* 7:3239–57

Kriest I, Evans GT. 1999. Representing phytoplankton aggregates in biogeochemical models. *Deep-Sea Res. Part I* 46:1841–59

Kriest I, Evans GT. 2000. A vertically resolved model for phytoplankton aggregation. *Proc. Indian Acad. Sci. Earth Planet. Sci.* 109:453–69

Lampitt RS. 1992. The contribution of deep-sea macroplankton to organic remineralization: results from sediment trap and zooplankton studies over the Madeira Abyssal Plain. *Deep-Sea Res. Part I* 39:221–33

Lampitt RS, Wishner KF, Turley CM, Angel MV. 1993. Marine snow studies in the northeast Atlantic Ocean: distribution, composition and role as a food source for migrating plankton. *Mar. Biol.* 116:689–702

Latimer P. 1985. Experimental tests of a theoretical method for predicting light-scattering by aggregates. *Appl. Opt.* 24:3231–39

Legendre L, Michaud J. 1998. Flux of biogenic carbon in oceans: size-dependent regulation by pelagic food webs. *Mar. Ecol. Prog. Ser.* 164:1–11

Le Quere C, Harrison SP, Prentice IC, Buitenhuis ET, Aumont O, et al. 2005. Ecosystem dynamics based on plankton functional types for global ocean biogeochemistry models. *Glob. Change Biol.* 11:2016–40

Loisel H, Nicolas JM, Sciandra A, Stramski D, Poteau A. 2006. Spectral dependency of optical backscattering by marine particles from satellite remote sensing of the global ocean. *J. Geophys. Res. Oceans* 111:C09O24

Lutz M, Dunbar R, Caldeira K. 2002. Regional variability in the vertical flux of particulate organic carbon in the ocean interior. *Glob. Biogeochem. Cycles* 16:1037

Martin ES, Harris RP, Irigoien X. 2006. Latitudinal variation in plankton size spectra in the Atlantic Ocean. *Deep-Sea Res. Part I* 53:1560–72

Martin JH, Knauer GA, Karl DM, Broenkow WW. 1987. VERTEX: carbon cycling in the Northeast Pacific. *Deep-Sea Res. Part I* 34:267–85

Maury O, Faugeras B, Shin YJ, Poggiale JC, Ben Ari T, Marsac F. 2007. Modeling environmental effects on the size-structured energy flow through marine ecosystems. Part 1: the model. *Prog. Oceanogr.* 74:479–99

McCave IN. 1983. Particulate size spectra, behavior, and origin of nepheloid layers over the Nova Scotian continental rise. *J. Geophys. Res.* 88:7647–66

McCave IN. 1984. Size spectra and aggregation of suspended particles in the deep ocean. *Deep-Sea Res. Part I* 31:329–52

McDonnell AMP, Buesseler KO. 2010. Variability in the average sinking velocity of marine particles. *Limnol. Oceanogr.* 55:2085–96

Mikkelsen OA, Hill PS, Milligan TG. 2006. Single-grain, microfloc and macrofloc volume variations observed with a LISST-100 and a digital floc camera. *J. Sea Res.* 55:87–102

Milligan TG. 1996. In situ particle (floc) size measurements with the Benthos 373 plankton silhouette camera. *J. Sea Res.* 36:93–100

Moore AM, Arango HG, Di Lorenzo E, Cornuelle BD, Miller AJ, Neilson DJ. 2004. A comprehensive ocean prediction and analysis system based on the tangent linear and adjoint of a regional ocean model. *Ocean Model.* 7:227–58

Morel A, Bricaud A. 1981. Theoretical results concerning light absorption in a discrete medium, and application to specific absorption of phytoplankton. *Deep-Sea Res.* 28:1375–93

Moutin T, Van Wambeke F, Prieur L. 2011. The Biogeochemistry from the Oligotrophic to the Ultraoligotrophic Mediterranean (BOUM) experiment. *Biogeosci. Discuss.* 8:8091–160

Olson RJ, Sosik HM. 2007. A submersible imaging-in-flow instrument to analyze nano- and microplankton: Imaging FlowCytobot. *Limnol. Oceanogr. Methods* 5:195–203

Picheral M, Guidi L, Stemmann L, Karl DM, Iddaoud G, Gorsky G. 2010. The Underwater Vision Profiler 5: an advanced instrument for high spatial resolution studies of particle size spectra and zooplankton. *Limnol. Oceanogr. Methods* 8:462–73

Platt T, Denman K. 1978. The structure of pelagic marine ecosystems. *J. Cons. Int. Explor. Mer.* 173:60–65
Ploug H. 2001. Small-scale oxygen fluxes and remineralization in sinking aggregates. *Limnol. Oceanogr.* 46:1624–31
Ploug H, Grossart HP. 2000. Bacterial growth and grazing on diatom aggregates: respiratory carbon turnover as a function of aggregate size and sinking velocity. *Limnol. Oceanogr.* 45:1467–75
Ploug H, Iversen MH, Fischer G. 2008a. Ballast, sinking velocity, and apparent diffusivity within marine snow and zooplankton fecal pellets: implications for substrate turnover by attached bacteria. *Limnol. Oceanogr.* 53:1878–86
Ploug H, Iversen MH, Koski M, Buitenhuis ET. 2008b. Production, oxygen respiration rates, and sinking velocity of copepod fecal pellets: direct measurements of ballasting by opal and calcite. *Limnol. Oceanogr.* 53:469–76
Pomeroy LR, Deibel D. 1980. Aggregation of organic matter by pelagic tunicates. *Limnol. Oceanogr.* 25:643–52
Ratmeyer V, Wefer G. 1996. A high resolution camera system (ParCa) for imaging particles in the ocean: system design and results from profiles and a three-month deployment. *J. Mar. Res.* 54:589–603
Riebessel U, Wolf-Gladrow DA. 1992. The relationship between physical aggregation of phytoplankton and vertical flux: a numerical model. *Deep-Sea Res. Part I* 39:1085–102
Riley GA, Bumpus DF. 1946. Phytoplankton-zooplankton relationships on Georges Bank. *J. Mar. Res.* 6:33–47
Riley GA, Stommel H, Bumpus F. 1949. Quantitative ecology of the plankton of the western North Atlantic. *Bull. Bingham Oceanogr. Coll.* 12:1–169
Sarmiento JL, Le Quere C. 1996. Oceanic carbon dioxide uptake in a model of century-scale global warming. *Science* 274:1346–50
Schmitt FG, Seuront L. 2001. Multifractal random walk in copepod behavior. *Phys. A* 301:375–96
Schmitt FG, Seuront L, Hwang JS, Souissi S, Tseng LC. 2006. Scaling of swimming sequences in copepod behavior: data analysis and simulation. *Phys. A* 364:287–96
Sheldon RW, Sutcliff Wh, Prakash A. 1972. Size distribution of particles in ocean. *Limnol. Oceanogr.* 17:327–40
Shifrin K. 1988. *Physical Optics of Ocean Water*. New York: AIP. 285 pp.
Sieracki CS, Sieracki ME, Yentsch CS. 1998. An imaging-in-flow system for automated analysis of marine microplankton. *Mar. Ecol. Prog. Ser.* 168:285–96
Silver MW, Coale SL, Pilskaln CH, Steinberg DR. 1998. Giant aggregates: importance as microbial centers and agents of material flux in the mesopelagic zone. *Limnol. Oceanogr.* 43:498–507
Silver MW, Gowing MM. 1991. The "particle" flux: origins and biological components. *Prog. Oceanogr.* 26:75–113
Silver MW, Gowing MM, Brownlee DC, Corliss JO. 1984. Ciliated protozoa associated with oceanic sinking detritus. *Nature* 309:246–48
Silver MW, Shanks AL, Trent JD. 1978. Marine snow—microplankton habitat and source of small-scale patchiness in pelagic populations. *Science* 201:371–73
Simon M, Grossart HP, Schweitzer B, Ploug H. 2002. Microbial ecology of organic aggregates in aquatic ecosystems. *Aquat. Microb. Ecol.* 28:175–211
Slade W, Boss E, Russo C. 2011. Effects of particle aggregation and disaggregation on their inherent optical properties. *Opt. Express* 19:7945–59
Smith DC, Simon M, Alldredge AL, Azam F. 1992. Intense hydrolytic enzyme activity on marine aggregates and implications for rapid particle dissolution. *Nature* 359:139–42
Smith KL Jr, Ruhl HA, Bett BJ, Billett DSM, Lampitt RS, Kaufmann RS. 2009. Climate, carbon cycling, and deep-ocean ecosystems. *Proc. Natl. Acad. Sci. USA* 106:19211–18
Sornes TA, Aksnes DL. 2004. Predation efficiency in visual and tactile zooplanktivores. *Limnol. Oceanogr.* 49:69–75
Sornes TA, Aksnes DL. 2006. Concurrent temporal patterns in light absorbance and fish abundance. *Mar. Ecol. Prog. Ser.* 325:181–86
Sornes TA, Hosia A, Bamstedt U, Aksnes DL. 2008. Swimming and feeding in *Periphylla periphylla* (Scyphozoa, Coronatae). *Mar. Biol.* 153:653–59
Sosik HM, Olson RJ, Neubert MG, Solow AR. 2003. Growth rates of coastal phytoplankton from time-series measurements with a submersible flow cytometer. *Limnol. Oceanogr.* 48:1756–65

Sprules WG, Jin EH, Herman AW, Stockwell JD. 1998. Calibration of an optical plankton counter for use in freshwater. *Limnol. Oceanogr.* 43:726–33

Sprules WG, Munawar M. 1986. Plankton size spectra in relation to ecosystem productivity, size and perturbation. *Can. J. Fish. Aquat. Sci.* 43:1789–94

Stemmann L, Eloire D, Sciandra A, Jackson GA, Guidi L, et al. 2008a. Volume distribution for particles between 3.5 to 2000 μm in the upper 200 m region of the South Pacific Gyre. *Biogeosciences* 5:299–310

Stemmann L, Gorsky G, Marty JC, Picheral M, Miquel JC. 2002. Four-year study of large-particle vertical distribution (0–1000 m) in the NW Mediterranean in relation to hydrology, phytoplankton, and vertical flux. *Deep-Sea Res. Part II* 49:2143–62

Stemmann L, Jackson GA, Gorsky G. 2004a. A vertical model of particle size distributions and fluxes in the midwater column that includes biological and physical processes—part II: application to a three year survey in the NW Mediterranean Sea. *Deep-Sea Res. Part I* 51:885–908

Stemmann L, Jackson GA, Ianson D. 2004b. A vertical model of particle size distributions and fluxes in the midwater column that includes biological and physical processes—part I: model formulation. *Deep-Sea Res. Part I* 51:865–84

Stemmann L, Picheral M, Gorsky G. 2000. Diel variation in the vertical distribution of particulate matter (>0.15 mm) in the NW Mediterranean Sea investigated with the Underwater Video Profiler. *Deep-Sea Res. Part I* 47:505–31

Stemmann L, Robert K, Hosia A, Picheral M, Paterson H, et al. 2008b. Global zoogeography of fragile macrozooplankton in the upper 100–1000 m inferred from the underwater video profiler. *ICES J. Mar. Sci.* 65:433–42

Stramski D, Boss E, Bogucki D, Voss KJ. 2004. The role of seawater constituents in light backscattering in the ocean. *Prog. Oceanogr.* 61:27–56

Suess E. 1980. Particulate organic-carbon flux in the oceans—surface productivity and oxygen utilization. *Nature* 288:260–63

Syvitski JPM, ed. 1991. *Principles, Methods and Applications of Particle Size Analysis*. New York: Cambridge Univ. Press. 368 pp.

Trent JD, Shanks AL, Silver MW. 1978. In situ and laboratory measurments on macroscopic aggregates in Monterey Bay, California. *Limnol. Oceonogr.* 23:626–35

Turley CM, Mackie PJ. 1994. Biogeochemical significance of attached and free-living bacteria and the flux of particles in the NE Atlantic Ocean. *Mar. Ecol. Prog. Ser.* 115:191–203

Twardowski MS, Boss E, Macdonald JB, Pegau WS, Barnard AH, Zaneveld JRV. 2001. A model for estimating bulk refractive index from the optical backscattering ratio and the implications for understanding particle composition in case I and case II waters. *J. Geophys. Res. Oceans* 106:14129–42

Van de Hulst H. 1981. *Light Scattering by Small Particles*. New York: Dover. 470 pp.

Vanderploeg HA, Roman MR. 2006. Introduction to special section on analysis of zooplankton distributions using the Optical Plankton Counter. *J. Geophys. Res. Oceans* 111:C05S01

Vidondo B, Prairie YT, Blanco JM, Duarte CM. 1997. Some aspects of the analysis of size spectra in aquatic ecology. *Limnol. Oceanogr.* 42:184–92

Visser AW, Kiørboe T. 2006. Plankton motility patterns and encounter rates. *Oecologia* 148:538–46

Visser AW, Saito H, Saiz E, Kiørboe T. 2001. Observations of copepod feeding and vertical distribution under natural turbulent conditions in the North Sea. *Mar. Biol.* 138:1011–19

Volk T, Hoffert MI. 1985. Ocean carbon pumps: analysis of relative strengths and efficiencies in ocean-driven atmospheric CO_2 changes. In *The Carbon Cycle and Atmospheric CO_2: Natural Variations Archean to Present*, ed. ET Sundquist, WS Broecker, pp. 99–110. Washington, DC: Am. Geophys. Union. 627 pp.

Volz F. 1954. Die Optik und Meterologie der atmosphärischen Trübung. *Ber. Deutch. Wetterdienstes* 2:3–47

Von Bertalanffy L. 1957. Quantitative laws in metabolism and growth. *Q. Rev. Biol.* 32:218–31

West GB, Savage VM, Gillooly J, Enquist BJ, Woodruff WH, Brown JH. 2003. Why does metabolic rate scale with body size? *Nature* 421:713

Woodward G, Ebenman B, Ernmerson M, Montoya JM, Olesen JM, et al. 2005. Body size in ecological networks. *Trends Ecol. Evol.* 20:402–9

Wyatt P, Jackson C. 1989. Discrimination of phytoplankton via light-scattering properties. *Limnol. Oceanog.* 34:96–112

Xu R. 2000. *Particle Characterization: Light Scattering Methods*. New York: Springer. 420 pp.
Yentsch C, Yentsch SC. 2008. Cell analysis in biological oceanography and its evolutionary implications. *J. Plankton Res.* 30:107–17
Zhang X, Twardowski M, Lewis M. 2011. Retrieving compostion and sizes of oceanic particle subpopulations from the volume scattering function. *Appl. Opt.* 50:1240–59
Zhou M. 2006. What determines the slope of a plankton biomass spectrum? *J. Plankton Res.* 28:437–48
Zhou M, Huntley ME. 1997. Population dynamics theory of plankton based on biomass spectra. *Mar. Ecol. Prog. Ser.* 159:61–73

Annual Review of
Marine Science

Volume 4, 2012

Contents

Errata

An online log of corrections to *Annual Review of Marine Science* articles may be found at http://marine.annualreviews.org/errata.shtml